

Temporal variation in the prokaryotic community of a nearshore marine environment

Marino Korlević^{1*}, Marsej Markovski¹, Gerhard J. Herndl^{2,3} and Mirjana Najdek¹

1. Center for Marine Research, Ruđer Bošković Institute, Croatia

2. Department of Functional and Evolutionary Ecology, University of Vienna, Austria

3. NIOZ, Department of Marine Microbiology and Biogeochemistry, Royal Netherlands Institute for Sea Research, Utrecht University, The Netherlands

*To whom correspondence should be addressed:

Marino Korlević

G. Paliaga 5, 52210 Rovinj, Croatia

Tel.: +385 52 804 768

Fax: +385 52 804 780

e-mail: marino.korlevic@irb.hr

Running title: Temporal variation in a nearshore prokaryotic community

1 Abstract

2 Prokaryotic communities inhabiting surface waters of temperate areas exhibit patterns of
3 seasonal succession. Studies describing these temporal changes are usually not performed at stations
4 located in the proximity to the coast. The temporal variation of these communities was determined
5 in the surface waters at two stations located in the close proximity to the eastern shore in the northern
6 Adriatic Sea. Sequencing of the V4 region of the 16S rRNA gene identified highest community
7 richness in December with distinct shifts in the community structure between spring, summer and
8 autumn/winter. Temperature was shown to be the main environmental force explaining community
9 temporal variation. *Synechococcus*, SAR86 clade, NS5 marine group and *Cryomorphaceae* were
10 detected throughout the seasonal cycle. In contrast, the spring community was characterized
11 by the NS4 marine group, *Formosa* and *Rhodobacteraceae*, the summer community by SAR11
12 subclades II and III, HIMB11, AEGEAN-169 marine group, OM60 (NOR5) clade and *Litoricola*
13 and the autumn/winter community by SAR11 subclade Ia and *Archaea*. Taken together, prokaryotic
14 communities inhabiting nearshore surface waters exhibit a general pattern in community composition
15 similar to other surface associated assemblages. However, certain characteristic season-specific
16 community structures and temporal patterns of specific taxonomic groups differ from other coastal
17 areas.

18 **Introduction**

19 Prokaryotic picoplankton communities inhabiting marine surface waters exhibit a seasonal
20 succession. These temporal community changes were described for surface waters of polar,
21 temperate and (sub)tropical regions (Bunse and Pinhassi, 2017). In temperate regions changes were
22 mainly associated with summer water column stratification, winter mixing and spring phytoplankton
23 blooms (Teeling et al., 2012; Bunse and Pinhassi, 2017; Mestre et al., 2020). Although general
24 successional patterns in these waters have been reported, some local differences were also observed.
25 While some studies have reported the exchange of multiple community states during the year
26 (Gilbert et al., 2009; Sintes et al., 2013; El-Swais et al., 2015; Lindh et al., 2015), others have
27 observed a community separation in only two major groups, specifically seasons (Mestre et al.,
28 2020), indicating that beside global patterns local environmental conditions may influence seasonal
29 community change.

30 Seasonal community variation in temperate waters usually starts with assemblages
31 characteristic for spring phytoplankton blooms. The successional pattern of different microbial
32 groups during the pre-bloom, bloom and bloom-decay periods have been described in detail
33 (Teeling et al., 2012, 2016; Sintes et al., 2013). The pre-bloom community is generally dominated
34 by members of the alphaproteobacterial SAR11 clade, during the bloom *Bacteroidota* taxa such as
35 *Formosa*, *Polaribacter*, *Ulvibacter* and the VIS6 clade become abundant while the decay period is
36 characterized by *Gammaproteobacteria*, i.e. the SAR92 clade (Teeling et al., 2012, 2016; Sintes
37 et al., 2013). Beside taxa co-occurring with phytoplankton blooms, communities specific to
38 summer water stratification and winter mixing were also described (Mestre et al., 2020). Usually,
39 *Cyanobacteria* are enriched during the summer, while some sub-clades of SAR11 are characteristic
40 for summer and some for winter months (Salter et al., 2015; Mestre et al., 2020).

41 The majority of studies describing temporal changes in temperate areas were performed at
42 long-term time series stations, such as the L4 sampling site of the Western Channel Observatory

43 (Gilbert et al., 2009, 2012), Blanes Bay Microbial Observatory (BBMO) (Alonso-Sáez et al., 2007;
44 Mestre et al., 2020), Linnaeus Microbial Observatory (Lindh et al., 2015), station Kabeltonne
45 in the German Bight (Teeling et al., 2012, 2016) and station E2 of the RADIALES time-series
46 project (Alonso-Sáez et al., 2015). Data obtained from such time-series studies have found that
47 a set of abiotic and biotic factors drive the temporal community variation (Bunse and Pinhassi,
48 2017). It was suggested that biological interactions primarily affect microbial dynamics over time
49 periods of days to weeks, while physicochemical parameters are mainly responsible for observed
50 seasonal successional patterns (Gilbert et al., 2009; Fuhrman et al., 2015; Needham and Fuhrman,
51 2016; Bunse and Pinhassi, 2017; Mestre et al., 2020). In addition, several studies indicate that
52 phytoplankton derived dissolved organic matter (DOM) drives community dynamics (Teeling et
53 al., 2012, 2016; Lindh et al., 2015; Needham and Fuhrman, 2016; Bunse and Pinhassi, 2017). It is
54 therefore worth investigating whether such general interactions also apply to nearshore microbial
55 communities.

56 To describe the temporal variation of microbial communities located in the proximity of the
57 shore and to disentangle the environmental variables responsible for their temporal change it is
58 important to apply a high-frequency sampling approach. Monthly sampling of surface waters at
59 two stations along the eastern coast of the northern Adriatic Sea was performed to determine the
60 temporal variation of prokaryotic picoplankton communities in these habitats. In addition, to assess
61 the main environmental parameters associated with community changes, compositional data were
62 linked to a set of previously reported environmental parameters measured at the same time (Najdek
63 et al., 2020a, 2020b).

64 **Materials and methods**

65 **Sampling**

66 Surface seawater from the northern Adriatic Sea was collected in the proximity of the shore
67 (25 – 50 m distance) in two bays ~7 km apart from each other, Saline (45°7'5'' N, 13°37'20'' E)
68 and Funtana (45°10'39'' N, 13°35'42'' E), by diving (depth, ~1.5 m). Samples were collected
69 in 10 l containers and transported to the laboratory where 10 – 20 l were filtered through a 20
70 µm mesh. The filtrate was further sequentially filtered using a peristaltic pump through 3 µm
71 and 0.2 µm polycarbonate membrane filters (Whatman, United Kingdom). Filters were dried
72 briefly at room temperature and stored at –80 °C. Samples were collected monthly from July 2017
73 to October 2018. Concurrently of sampling for picoplankton community structure assessment,
74 additional samples were collected to determine environmental parameters (temperature, salinity,
75 orthophosphate, ammonium, nitrite, nitrate, orthosilicate, particulate matter, chlorophyll *a* and
76 prokaryotic abundance) as reported previously (Najdek et al., 2020a, 2020b).

77 **DNA isolation**

78 Picoplankton DNA was isolated from 0.2 µm polycarbonate filters according to Massana et
79 al. (1997) with slight modifications. Following phenol-chloroform extractions, 1/10 of 3 M chilled
80 sodium acetate (pH 5.2) was added. DNA was precipitated by the addition of 1 volume of chilled
81 isopropanol, incubating the mixtures overnight at –20 °C and centrifuging at 20,000 × g and 4 °C
82 for 21 min. Pellets were washed twice with 500 µl of 70 % chilled ethanol and centrifuged after
83 each washing step at 20,000 × g and 4 °C for 5 min. Air-dried pellets were re-suspended in 50 µl of
84 deionized water.

85 **Illumina 16S rRNA sequencing**

86 The V4 region of the gene for 16S rRNA was sequenced using the Illumina MiSeq platform
87 as described previously (Korlević et al., submitted). A two-step PCR procedure was applied to
88 amplify the target region. In the first PCR, primers 515F (5'-GTGYCAGCMGCCGCGTAA-3')
89 and 806R (5'-GGACTACNVGGTWTCTAAT-3') from the Earth Microbiome Project (<https://earthmicrobiome.org/protocols-and-standards/16s/>) were used (Caporaso et al., 2012; Apprill
90 et al., 2015; Parada et al., 2016). Tagged sequences were added to these primers on their 5'
91 end. PCR products were purified and sent for Illumina MiSeq sequencing at IMGM Laboratories,
92 Martinsried, Germany. Prior to sequencing at IMGM, adapter and sample-specific index sequences
93 were incorporated during the second PCR amplification of the two-step PCR procedure using
94 primers targeting the tagged region. Beside samples, a positive and a negative control were included
95 in each sequencing batch. For the positive control a mock community consisting of evenly mixed
96 DNA material originating from 20 bacterial strains (ATCC MSA-1002, ATCC, USA) was used,
97 while the negative control comprised PCR reactions without DNA template. Reads obtained in
98 this study (Bay of Saline) were combined with reads previously reported in a study describing
99 temporal dynamics of surface associated microbial communities (Bay of Funtana) (Korlević et al.,
100 submitted) and analysed together. Sequences processed in this study have been deposited in the
101 European Nucleotide Archive (ENA) at EMBL-EBI under accession numbers SAMEA6648771 –
102 SAMEA6648788, SAMEA6648824, SAMEA6648825, SAMEA8117500 – SAMEA8117516.
103

104 **Sequence analysis**

105 Sequences obtained in the present study were analysed using mothur (version 1.43.0) (Schloss
106 et al., 2009) according to the MiSeq Standard Operating Procedure (MiSeq SOP; https://mothur.org/wiki/MiSeq_SOP) (Kozich et al., 2013) and recommendations given by the Riffomonas project
107 to enhance data reproducibility (<http://www.riffomonas.org/>). Sequences were clustered into
108

109 operational taxonomic units (OTUs) at a similarity level of 97 % as suggested by the MiSeq
110 SOP. Computing was performed on the computer cluster Isabella (University Computing Center,
111 University of Zagreb). Alignment and classification was performed using the SILVA SSU Ref
112 NR 99 database (release 138; <http://www.arb-silva.de>) (Quast et al., 2013; Yilmaz et al., 2014).
113 Pipeline data processing and visualisation was done using R (version 3.6.0) (R Core Team, 2019) in
114 combination with packages vegan (version 2.5.6) (Oksanen et al., 2019), tidyverse (version 1.2.1)
115 (Wickham, 2017; Wickham et al., 2019) and multiple other packages (Neuwirth, 2014; Xie, 2014,
116 2015, 2019a, 2019b, 2019c; Xie et al., 2018; Allaire et al., 2019; McKinnon Edwards, 2019; Wilke,
117 2019; Zhu, 2019). The detailed analysis procedure including the RMarkdown file are available in
118 the GitHub repository (https://github.com/MicrobesRovinj/Korlevic_SeawaterDynamics_x_2021).
119 The average sequencing error rate of 0.01 % was calculated based on the ATCC MSA-1002 mock
120 community included in each sequencing batch, which is in line with previously reported values for
121 next-generation 16S rRNA amplicon sequencing (Kozich et al., 2013; Schloss et al., 2016). Also,
122 negative controls processed together with the samples yielded on average only 2 sequences after
123 quality curation.

124 **Results**

125 Sequencing of 17 samples from the Bay of Saline and 18 samples from the Bay of Funtana
126 (one of the samples was a sequencing replicate) yielded 1.5 million reads after quality curation and
127 exclusion of sequences without known relatives (no relative sequences), eukaryotic, chloroplast and
128 mitochondrial sequences (Table S1). The number of reads per sample ranged from 25,360 to 77,466
129 (Fig. S1 and Table S1). Reads were clustered into 16,629 different OTUs at a similarity level of 97
130 %. To account for different sequencing depth reads were normalized to the minimum number of
131 sequences per sample (25,360, Table S1) that resulted in 13,440 different OTUs ranging from 608
132 to 1,790 OTUs per sample (Fig. S2).

133 Temporal variations in richness and diversity were determined by calculating the observed
134 number of OTUs, Chao1, ACE, Exponential Shannon and Inverse Simpson index (Jost, 2006).
135 Similar trends in richness and diversity were observed at both stations (Fig. S2) characterized by
136 a maximum richness in both, the Saline (Number of OTUs, 1,790 OTUs) and Funtana (Number
137 of OTUs, 1,786 OTUs) Bay in December 2017. In contrast, the Inverse Simpson index did not
138 show an elevated value in December 2017 indicating that rare OTUs contributed substantially
139 to the observed richness maxima. To determine temporal changes in the proportion of shared
140 OTUs and in communities the Jaccard's and Bray-Curtis similarity coefficients were calculated
141 between consecutive sampling points (Fig. S3). Similar trends were observed at both stations
142 with higher stability of shared bacterial and archaeal OTUs (Jaccard's similarity coefficient) than
143 community similarity (Bray-Curtis similarity coefficient). A substantial decline in community
144 similarity between March and April 2018 was observed at both stations indicating a pronounced
145 community shift in this period (Fig. S3). Analysis of this time series data showed that only 0.3 % of
146 OTUs were present throughout the study period while these persistent OTUs contributed to 62.0 %
147 of sequences.

148 To evaluate the temporal variation of bacterial and archaeal communities Principal Coordinate

149 Analysis (PCoA) of Bray-Curtis distances was applied to the OTU community data (Fig. 1A).
150 Communities specific to summer, autumn/winter and spring could be identified regardless of the
151 station sampled. This separation in three specific communities was further supported by ANOSIM
152 ($R = 0.72$, $p < 0.01$). To assess which environmental parameter mainly contributes to the observed
153 temporal community variation, the community data were constrained by a set of previously reported
154 environmental variables (Najdek et al., 2020a, 2020b) using Distance-Based Redundancy Analysis
155 (db-RDA) (Fig. 1B). Nearly half ($R^2_a = 45.5\%$) of the observed community variation could be
156 explained by the variables. Separation between summer and autumn/winter communities was
157 mainly explained by temperature, prokaryotic abundance, salinity and nitrite. In contrast, neither
158 variable could strongly explain the spring community composition.

159 The classification of reads showed that the prokaryotic community was dominated by bacterial
160 ($98.3 \pm 3.5\%$) over archaeal sequences ($1.7 \pm 3.5\%$) (Fig. 2). A higher relative contribution of
161 archaeal reads was observed only in November 2017 ($7.5 \pm 2.2\%$), December 2017 ($13.2 \pm 1.4\%$)
162 and February 2018 ($3.7 \pm 0.9\%$). The main taxonomic groups contributing to the higher relative
163 abundance of *Archaea* in this period were the *Crenarchaeota* “*Candidatus Nitrosopumilus*” and
164 the *Thermoplasmatota* Marine group II. The bacterial community was comprised of well-known
165 seawater groups such as the *Actinobacteriota*, *Bacteroidota*, *Cyanobacteria*, *Marinimicrobia*,
166 *Alphaproteobacteria*, *Gammaproteobacteria* and *Verrucomicrobiota* (Fig. 2). Generally, similar
167 temporal patterns were observed at both stations.

168 *Cyanobacteria* comprised on average $5.1 \pm 2.8\%$ of the prokaryotic community. The highest
169 relative contribution was recorded in winter ($8.2 \pm 5.6\%$), mainly caused by the high proportion
170 in March 2018 ($13.0 \pm 1.6\%$) (Fig. 2). The cyanobacterial community was largely dominated by
171 *Synechococcus*, especially during periods of higher cyanobacterial presence (Fig. 3). *Bacteroidota*
172 comprised on average $21.8 \pm 6.2\%$ of the community. Slightly higher values were found in
173 spring and summer ($23.9 \pm 4.6\%$) than in autumn and winter ($18.0 \pm 7.1\%$) (Fig. 2). Although
174 *Bacteroidota* showed only slight temporal variations, taxa within this group exhibited strong seasonal

175 patterns (Fig. 4). Groups such as the NS5 marine group and uncultured *Cryomorphaceae* were
176 present throughout the year, while sequences classified as *Balneola*, uncultured *Balneolaceae* and
177 the NS11-12 marine group were more pronounced from May to October. In addition, *Formosa* and
178 the NS4 marine group could be detected throughout the study period but specifically contributed to
179 the *Bacteroidota* community in March and April 2018, respectively. Higher values of chloroplast
180 sequences were also recorded at this time (Fig. S4). In addition, while uncultured *Saprospiraceae*
181 from the Saline Bay samples contributed substantially to the *Bacteroidota* community in June and
182 July 2018, they were not abundant in Funtana Bay (Fig. 4).

183 Sequences classified as *Alphaproteobacteria* showed the highest relative abundance and
184 comprised on average $38.3 \pm 8.0\%$ of the prokaryotic community (Fig. 2). The relative contribution
185 of *Alphaproteobacteria* was higher in summer ($41.3 \pm 6.3\%$) and winter ($44.0 \pm 2.2\%$) than in
186 autumn ($34.9 \pm 4.9\%$) and spring ($31.1 \pm 11.5\%$). The temporal variation of taxa within this class
187 showed a more complex pattern (Fig. 5). The most pronounced community shift was observed
188 in April 2018 when reads of the usually prominent SAR11 clade were scarce and *Stappiaceae*,
189 *Ascidiaeihabitans* and no relative *Rhodobacteraceae* dominated the alphaproteobacterial
190 community. Subclades within SAR11 also showed temporal patterns. Subclades II and III
191 characterized the SAR11 community in summer from June to September, while from November
192 to March reads classified as subclade Ia comprised the majority of SAR11-specific sequences.
193 Except of the SAR11 subclades II and III, summer months were also characterized by two other
194 alphaproteobacterial groups, the HIMB11 and the AEGEAN-169 marine group (Fig. 5).

195 Reads classified as *Gammaproteobacteria* comprised on average $21.6 \pm 6.6\%$ of the
196 prokaryotic community (Fig. 2). The season with the the highest relative contribution of
197 gammaproteobacterial sequences was spring ($29.9 \pm 12.3\%$), while in other seasons values ranged
198 from 18.9 ± 2.6 to $22.3 \pm 2.5\%$. Within the *Gammaproteobacteria*, the SAR86 clade was present
199 throughout the year while other taxa were season-specific, such as *Litoricola*, the OM60 (NOR5)
200 clade and the SUP05 cluster (Fig. 6). *Litoricola* and the OM60 (NOR5) clade characterized

201 the gammaproteobacterial community from April to August, while sequences specific for the
202 SUP05 cluster were detected from November to March. Taxonomic groups of high-level bacterial
203 taxa that comprised a lower proportion of prokaryotic sequences such as the *Actinobacteriota*
204 and *Verrucomicrobiota* also showed temporal variations. During the period of higher relative
205 sequence abundance of *Actinobacteriota*, between September and December, the actinobacterial
206 community was comprised mainly of “*Candidatus Actinomarina*”. Similarly, in April and May
207 when *Verrucomicrobiota* specific reads exhibited the highest relative abundance, *Lentimonas* and
208 *Coraliomargarita* were the main constituent of the *Verrucomicrobiota*.

209 **Discussion**

210 Prokaryotic communities inhabiting surface waters of temperate and (sub)polar regions exhibit
211 patterns of seasonal succession (Bunse and Pinhassi, 2017). These temporal variations were mainly
212 studied at long-term time series sites usually encompassing only one sampling station located further
213 away from the coast (Gilbert et al., 2009; Mestre et al., 2020). In the present study the temporal
214 variation of surface prokaryotic communities was determined at two sites in the close proximity of
215 the shore. Similar patterns were observed at both sites indicating that the observed pattern might be
216 representative for surface waters of a wider area.

217 Temporal changes in richness were considerable as indicated by the low proportion of OTUs
218 present at each sampling date (0.3 %). This low number of persistent OTUs, however, comprised a
219 high proportion of reads (62.0 %). Similar proportions of persistent core OTUs and their contribution
220 to the total number of sequences were also reported in other time series studies (Gilbert et al., 2009,
221 2012). Analysis of the temporal variations in alpha-diversity showed maximal richness in December
222 (Fig. S2). This observation is in agreement with previously reported richness maxima in other
223 regions during colder months (Gilbert et al., 2012; Ladau et al., 2013; El-Swais et al., 2015;
224 Mestre et al., 2020). It has been suggested that late autumn/winter overturn is responsible for this
225 phenomenon by simply mixing populations from deeper parts of the water column with existing
226 ones (García et al., 2015; Salter et al., 2015; Bunse and Pinhassi, 2017). However, a similar richness
227 pattern was also observed in regional seas where seasonal overturning of the water column does
228 not play a role, such as in the shallow North Sea where also a higher richness was observed in
229 winter (Reinthalter et al., 2005). Although the samples in this study were retrieved at very shallow
230 locations, water column mixing taking place at deeper areas could bring additional taxa to these
231 locations causing the observed increase in alpha-diversity.

232 The majority of studies analysing temporal community variation usually identified an exchange
233 of multiple community states during the year (El-Swais et al., 2015; Lindh et al., 2015). In contrast,

some studies described only a switch between winter- and summer-specific assemblages (Ward et al., 2017; Mestre et al., 2020). These differences might be a consequence of local conditions. Indeed, some studies attributed the observed lower number of assemblages to the absence of large spring and fall phytoplankton blooms in some areas (Ward et al., 2017). We identified three distinct microbial assemblages characteristic for spring, summer and autumn/winter (Fig. 1A). This is in agreement with studies describing the exchange of multiple communities over an annual cycle with a distinct spring community assemblage (El-Swais et al., 2015; Lindh et al., 2015). The distinct spring community we detected is likely a response to a phytoplankton bloom that can occur in this region (Mozetič et al., 2010; Manna et al., 2021). Temperature and prokaryotic abundance were identified as main factors influencing the exchange of communities between the summer and autumn/winter period (Fig. 1B). It is not surprising that temperature and prokaryotic abundance are equally explaining this shift as higher prokaryotic abundances were reported in this area during summer months (Ivančić et al., 2010). The identification of temperature as the single most important driver of community change is in line with previously reported data (El-Swais et al., 2015; Ward et al., 2017; Mestre et al., 2020). It was proposed that temperature indirectly influences community change through phytoplankton nutrient limitation during water column stratification and nutrient input in times of water column mixing (Bunse and Pinhassi, 2017). Factors explaining the onset of a separate spring community were not identified. We hypothesise that based on a slightly higher value of chloroplast specific reads in these samples and the presence of taxa specific for phytoplankton blooms this community was a late prokaryotic response to a phytoplankton bloom even though the concentration of chlorophyll *a* could not explain it.

Differences between communities specific for spring, summer and autumn/winter observed at the level of OTUs could also be seen in the taxonomic composition (Figs. 2 – 6). The identified spring-specific community contained taxa previously associated with phytoplankton blooms (Figs. 4 and 5) (Teeling et al., 2012, 2016; Sintes et al., 2013). *Formosa* and members within the *Rhodobacteraceae* were associated with phytoplankton blooms in the North Sea (Teeling et al., 2012, 2016), while the NS4 marine group was found in previous studies describing bacterial communities

261 in different environments of the Adriatic Sea with no clear association with increased autotrophic
262 biomass (Korlević et al., 2015, 2016). Observed variations in spring communities between different
263 areas could be explained by differences in structure and supply of phototroph-derived organic matter.
264 The summer community was characterized by the family *Balneolaceae* and the NS11-12 marine
265 group from the *Bacteroidota*, the SAR11 subclades II and III, HIMB11 and the AEGEAN-169
266 marine group from the *Alphaproteobacteria* and from the *Gammaproteobacteria* the OM60 (NOR5)
267 clade and *Litoricola* (Figs. 4 – 6). In contrast, the winter community was characterized by
268 the archaeal “*Candidatus Nitrosopumilus*” and Marine group II, the alphaproteobacterial SAR11
269 subclade Ia and the gammaproteobacterial SUP05 cluster (Figs. 2, 5 and 6). Temporal and
270 depth-related variation of different SAR11 subclades was also reported previously although we
271 observed a different pattern in comparison to other surface associated SAR11 communities (Carlson
272 et al., 2009; Vergin et al., 2013; Salter et al., 2015). In contrast to these former studies, we
273 observed a higher contribution of the SAR11 subclade Ia to the community in the winter. A higher
274 contribution of members in the summer community such as the HIMB11, the OM60 (NOR5) clade
275 and *Litoricola* could result from their adaptation to more oligotrophic conditions during water
276 column stratification in summer through the ability to use alternative pathways of energy supply
277 (i.e. bacteriochlorophyll and proteorhodopsin) (Huggett and Rappe, 2012; Spring and Riedel, 2013;
278 Durham et al., 2014). A study describing a strong co-dominance of “*Candidatus Nitrosopumilus*”
279 and Marine group II suggests that nitrification by ammonia-oxidising archaea is coupled with
280 ammonification performed by the members of the Marine group II (Kim et al., 2019). In addition,
281 the presence of “*Candidatus Nitrosopumilus*” reads in our samples is not surprising as recently two
282 new strains of ammonia-oxidising archaea within the genus *Nitrosopumilus* have been isolated from
283 northern Adriatic coastal waters (Bayer et al., 2019).

284 Beside groups exhibiting specificity to one of the identified temporal communities,
285 ubiquitous taxa were detected, such as *Synechococcus*, the flavobacterial NS5 marine group and
286 *Cryomorphaceae* and the gammaproteobacterial SAR86 clade (Figs. 3, 4 and 6). The dominance
287 of *Synechococcus* over other cyanobacterial groups in this coastal area was reported previously

(Šilović et al., 2012; Tinta et al., 2015). The known genome versatility of *Synechococcus* could explain the high contribution of this genus to the cyanobacterial community in fluctuating coastal environments (Palenik et al., 2003). The *Cryomorphaceae* are associated with organic matter remineralisation processes (Bowman, 2014), while a single-cell genome analysis of the NS5 marine group revealed the ability to degrade marine polysaccharides (Ngugi and Stingl, 2018). In addition, the NS5 marine group was previously detected in different seasons and environments of the Adriatic Sea (Korlević et al., 2015, 2016). These two groups are part of a basic remineralisation community present at this location throughout the year. The gammaproteobacterial SAR86 clade, previously reported in different environments of the Adriatic Sea (Korlević et al., 2015, 2016; Tinta et al., 2015), was also detected throughout the year. Recent analysis of metagenomic data suggests the existence of different functional and ecological ecotypes of this ubiquitous clade (Hoarfrost et al., 2020). It is possible that different ecotypes are also characteristic for different seasons.

In conclusion, prokaryotic communities inhabiting the proximity of the shore exhibit temporal variations similar to surface water assemblages in other temperate regions. As in other regions, a richness maximum was recorded in the colder period of the year and seasonal community shifts were observed. Temperature was identified as the main force driving seasonal community change. Besides these similarities, temporal analysis of taxonomic data identified a season-specific community structure and groups exhibiting temporal patterns different from other coastal areas indicating that beside global driving factors local conditions also influence the coastal prokaryotic community.

308 **Acknowledgments**

309 This study was funded by the Croatian Science Foundation through the MICRO-SEAGRASS
310 project (project number IP-2016-06-7118). GJH was supported by the Austrian Science Fund
311 (FWF) through the ARTEMIS project (project number P28781-B21). We would like to thank the
312 University Computing Center of the University of Zagreb for access to the computer cluster Isabella,
313 Margareta Buterer for technical support and Paolo Paliaga for help during sampling.

314 **References**

- 315 Allaire, J. J., Xie, Y., McPherson, J., Luraschi, J., Ushey, K., Atkins, A., et al. (2019).
- 316 *rmarkdown: Dynamic documents for R.*
- 317 Alonso-Sáez, L., Balagué, V., Sà, E. L., Sánchez, O., González, J. M., Pinhassi, J., et
318 al. (2007). Seasonality in bacterial diversity in north-west Mediterranean coastal waters:
319 Assessment through clone libraries, fingerprinting and FISH. *FEMS Microbiol. Ecol.* 60, 98–112.
320 doi:10.1111/j.1574-6941.2006.00276.x.
- 321 Alonso-Sáez, L., Díaz-Pérez, L., and Morán, X. A. G. (2015). The hidden seasonality of
322 the rare biosphere in coastal marine bacterioplankton. *Environ. Microbiol.* 17, 3766–3780.
323 doi:10.1111/1462-2920.12801.
- 324 Apprill, A., McNally, S., Parsons, R., and Weber, L. (2015). Minor revision to V4 region SSU
325 rRNA 806R gene primer greatly increases detection of SAR11 bacterioplankton. *Aquat. Microb.
326 Ecol.* 75, 129–137. doi:10.3354/ame01753.
- 327 Bayer, B., Vojvoda, J., Reinthaler, T., Reyes, C., Pinto, M., and Herndl, G. J. (2019).
328 *Nitrosopumilus adriaticus* sp. nov. and *Nitrosopumilus piranensis* sp. nov., two ammonia-oxidizing
329 archaea from the Adriatic Sea and members of the class *Nitrososphaeria*. *Int. J. Syst. Evol.
330 Microbiol.* 69, 1892–1902. doi:10.1099/ijsem.0.003360.
- 331 Bowman, J. P. (2014). “The family *Cryomorphaceae*,” in *The Prokaryotes: Other
332 Major Lineages of Bacteria and the Archaea*, eds. E. Rosenberg, E. F. DeLong, S. Lory,
333 E. Stackebrandt, and F. Thompson (Berlin, Heidelberg: Springer-Verlag), 539–550.
334 doi:10.1007/978-3-642-38954-2_135.
- 335 Bunse, C., and Pinhassi, J. (2017). Marine bacterioplankton seasonal succession dynamics.
336 *Trends Microbiol.* 25, 494–505. doi:10.1016/j.tim.2016.12.013.

- 337 Caporaso, J. G., Lauber, C. L., Walters, W. A., Berg-Lyons, D., Huntley, J., Fierer, N., et al.
338 (2012). Ultra-high-throughput microbial community analysis on the Illumina HiSeq and MiSeq
339 platforms. *ISME J.* 6, 1621–1624. doi:10.1038/ismej.2012.8.
- 340 Carlson, C. A., Morris, R., Parsons, R., Treusch, A. H., Giovannoni, S. J., and Vergin, K.
341 (2009). Seasonal dynamics of SAR11 populations in the euphotic and mesopelagic zones of the
342 northwestern Sargasso Sea. *ISME J.* 3, 283–295. doi:10.1038/ismej.2008.117.
- 343 Durham, B. P., Grote, J., Whittaker, K. A., Bender, S. J., Luo, H., Grim, S. L., et al.
344 (2014). Draft genome sequence of marine alphaproteobacterial strain HIMB11, the first cultivated
345 representative of a unique lineage within the *Roseobacter* clade possessing an unusually small
346 genome. *Stand. Genomic Sci.* 9, 632–645. doi:10.4056/sigs.4998989.
- 347 El-Swais, H., Dunn, K. A., Bielawski, J. P., Li, W. K. W., and Walsh, D. A. (2015). Seasonal
348 assemblages and short-lived blooms in coastal north-west Atlantic Ocean bacterioplankton. *Environ.*
349 *Microbiol.* 17, 3642–3661. doi:10.1111/1462-2920.12629.
- 350 Fuhrman, J. A., Cram, J. A., and Needham, D. M. (2015). Marine microbial
351 community dynamics and their ecological interpretation. *Nat. Rev. Microbiol.* 13, 133–146.
352 doi:10.1038/nrmicro3417.
- 353 García, F. C., Alonso-Sáez, L., Morán, X. A. G., and López-Urrutia, Á. (2015). Seasonality in
354 molecular and cytometric diversity of marine bacterioplankton: The re-shuffling of bacterial taxa by
355 vertical mixing. *Environ. Microbiol.* 17, 4133–4142. doi:10.1111/1462-2920.12984.
- 356 Gilbert, J. A., Field, D., Swift, P., Newbold, L., Oliver, A., Smyth, T., et al. (2009). The
357 seasonal structure of microbial communities in the Western English Channel. *Environ. Microbiol.*
358 11, 3132–3139. doi:10.1111/j.1462-2920.2009.02017.x.

359 Gilbert, J. A., Steele, J. A., Caporaso, J. G., Steinbrück, L., Reeder, J., Temperton, B., et
360 al. (2012). Defining seasonal marine microbial community dynamics. *ISME J.* 6, 298–308.
361 doi:10.1038/ismej.2011.107.

362 Hoarfrost, A., Nayfach, S., Ladau, J., Yooseph, S., Arnosti, C., Dupont, C. L., et al.
363 (2020). Global ecotypes in the ubiquitous marine clade SAR86. *ISME J.* 14, 178–188.
364 doi:10.1038/s41396-019-0516-7.

365 Huggett, M. J., and Rappe, M. S. (2012). Genome sequence of strain HIMB30, a novel member
366 of the marine *Gammaproteobacteria*. *J. Bacteriol.* 194, 732–733. doi:10.1128/JB.06506-11.

367 Ivančić, I., Fuks, D., Najdek, M., Blažina, M., Devescovi, M., Šilović, T., et al. (2010).
368 Long-term changes in heterotrophic prokaryotes abundance and growth characteristics in the
369 northern Adriatic Sea. *J. Mar. Syst.* 82, 206–216. doi:10.1016/J.JMARSYS.2010.05.008.

370 Jost, L. (2006). Entropy and diversity. *Oikos* 113, 363–375.
371 doi:10.1111/j.2006.0030-1299.14714.x.

372 Kim, J.-G., Gwak, J.-H., Jung, M.-Y., An, S.-U., Hyun, J.-H., Kang, S., et al. (2019). Distinct
373 temporal dynamics of planktonic archaeal and bacterial assemblages in the bays of the Yellow Sea.
374 *PLoS One* 14, e0221408. doi:10.1371/journal.pone.0221408.

375 Korlević, M., Markovski, M., Zhao, Z., Herndl, G. J., and Najdek, M. Seasonal dynamics of
376 epiphytic microbial communities on marine macrophyte surfaces.

377 Korlević, M., Markovski, M., Zhao, Z., Herndl, G. J., and Najdek, M. Selective DNA and
378 protein isolation from marine macrophyte surfaces.

379 Korlević, M., Pop Ristova, P., Garić, R., Amann, R., and Orlić, S. (2015). Bacterial diversity
380 in the South Adriatic Sea during a strong, deep winter convection year. *Appl. Environ. Microbiol.*
381 81, 1715–1726. doi:10.1128/AEM.03410-14.

- 382 Korlević, M., Šupraha, L., Ljubešić, Z., Henderiks, J., Ciglenečki, I., Dautović, J., et al. (2016).
- 383 Bacterial diversity across a highly stratified ecosystem: A salt-wedge Mediterranean estuary. *Syst.*
- 384 *Appl. Microbiol.* 39, 398–408. doi:10.1016/j.syapm.2016.06.006.
- 385 Kozich, J. J., Westcott, S. L., Baxter, N. T., Highlander, S. K., and Schloss, P. D. (2013).
- 386 Development of a dual-index sequencing strategy and curation pipeline for analyzing amplicon
- 387 sequence data on the MiSeq Illumina sequencing platform. *Appl. Environ. Microbiol.* 79,
- 388 5112–5120. doi:10.1128/AEM.01043-13.
- 389 Ladau, J., Sharpton, T. J., Finucane, M. M., Jospin, G., Kembel, S. W., O'Dwyer, J., et al.
- 390 (2013). Global marine bacterial diversity peaks at high latitudes in winter. *ISME J.* 7, 1669–1677.
- 391 doi:10.1038/ismej.2013.37.
- 392 Lindh, M. V., Sjöstedt, J., Andersson, A. F., Baltar, F., Hugerth, L. W., Lundin, D., et al. (2015).
- 393 Disentangling seasonal bacterioplankton population dynamics by high-frequency sampling. *Environ.*
- 394 *Microbiol.* 17, 2459–2476. doi:10.1111/1462-2920.12720.
- 395 Manna, V., De Vittor, C., Giani, M., Del Negro, P., and Celussi, M. (2021). Long-term patterns
- 396 and drivers of microbial organic matter utilization in the northernmost basin of the Mediterranean
- 397 Sea. *Mar. Environ. Res.* 164, 105245. doi:10.1016/j.marenvres.2020.105245.
- 398 Massana, R., Murray, A. E., Preston, C. M., and DeLong, E. F. (1997). Vertical distribution
- 399 and phylogenetic characterization of marine planktonic *Archaea* in the Santa Barbara Channel. *Appl.*
- 400 *Environ. Microbiol.* 63, 50–56.
- 401 McKinnon Edwards, S. (2019). *lemon: Freshing up your 'ggplot2' plots.*
- 402 Mestre, M., Höfer, J., Sala, M. M., and Gasol, J. M. (2020). Seasonal variation of
- 403 bacterial diversity along the marine particulate matter continuum. *Front. Microbiol.* 11, 1590.
- 404 doi:10.3389/fmicb.2020.01590.

405 Mozetič, P., Solidoro, C., Cossarini, G., Socal, G., Precali, R., Francé, J., et al. (2010). Recent
406 trends towards oligotrophication of the Northern Adriatic: Evidence from chlorophyll *a* time series.
407 *Estuaries Coast* 33, 362–375. doi:10.1007/s12237-009-9191-7.

408 Najdek, M., Korlević, M., Paliaga, P., Markovski, M., Ivančić, I., Iveša, L., et al. (2020a).
409 Dynamics of environmental conditions during the decline of a *Cymodocea nodosa* meadow.
410 *Biogeosciences* 17, 3299–3315. doi:10.5194/bg-17-3299-2020.

411 Najdek, M., Korlević, M., Paliaga, P., Markovski, M., Ivančić, I., Iveša, L., et al. (2020b).
412 Effects of the invasion of *Caulerpa cylindracea* in a *Cymodocea nodosa* meadow in the Northern
413 Adriatic Sea. *Front. Mar. Sci.* 7, 602055. doi:10.3389/fmars.2020.602055.

414 Needham, D. M., and Fuhrman, J. A. (2016). Pronounced daily succession of
415 phytoplankton, archaea and bacteria following a spring bloom. *Nat. Microbiol.* 1, 1–7.
416 doi:10.1038/nmicrobiol.2016.5.

417 Neuwirth, E. (2014). *RColorBrewer: ColorBrewer palettes*.

418 Ngugi, D. K., and Stingl, U. (2018). High-quality draft single-cell genome sequence
419 of the NS5 marine group from the coastal Red Sea. *Genome Announc.* 6, e00565–18.
420 doi:10.1128/genomeA.00565-18.

421 Oksanen, J., Blanchet, F. G., Friendly, M., Kindt, R., Legendre, P., McGlinn, D., et al. (2019).
422 *vegan: Community ecology package*.

423 Palenik, B., Brahamsha, B., Larimer, F. W., Land, M., Hauser, L., Chain, P., et al. (2003). The
424 genome of a motile marine *Synechococcus*. *Nature* 424, 1037–1042. doi:10.1038/nature01943.

425 Parada, A. E., Needham, D. M., and Fuhrman, J. A. (2016). Every base matters: Assessing
426 small subunit rRNA primers for marine microbiomes with mock communities, time series and
427 global field samples. *Environ. Microbiol.* 18, 1403–1414. doi:10.1111/1462-2920.13023.

428 Quast, C., Pruesse, E., Yilmaz, P., Gerken, J., Schweer, T., Yarza, P., et al. (2013). The SILVA
429 ribosomal RNA gene database project: Improved data processing and web-based tools. *Nucleic
430 Acids Res.* 41, D590–D596. doi:10.1093/nar/gks1219.

431 R Core Team (2019). *R: A language and environment for statistical computing*. Vienna,
432 Austria: R Foundation for Statistical Computing.

433 Reinthaler, T., Winter, C., and Herndl, G. J. (2005). Relationship between bacterioplankton
434 richness, respiration, and production in the southern North Sea. *Appl. Environ. Microbiol.* 71,
435 2260–2266. doi:10.1128/AEM.71.5.2260-2266.2005.

436 Salter, I., Galand, P. E., Fagervold, S. K., Lebaron, P., Obernosterer, I., Oliver, M. J., et al.
437 (2015). Seasonal dynamics of active SAR11 ecotypes in the oligotrophic Northwest Mediterranean
438 Sea. *ISME J.* 9, 347–360. doi:10.1038/ismej.2014.129.

439 Schloss, P. D., Jenior, M. L., Koumpouras, C. C., Westcott, S. L., and Highlander, S. K. (2016).
440 Sequencing 16S rRNA gene fragments using the PacBio SMRT DNA sequencing system. *PeerJ* 4,
441 e1869. doi:10.7717/peerj.1869.

442 Schloss, P. D., Westcott, S. L., Ryabin, T., Hall, J. R., Hartmann, M., Hollister, E. B., et al.
443 (2009). Introducing mothur: Open-source, platform-independent, community-supported software
444 for describing and comparing microbial communities. *Appl. Environ. Microbiol.* 75, 7537–7541.
445 doi:10.1128/AEM.01541-09.

446 Sintes, E., Witte, H., Stodderegger, K., Steiner, P., and Herndl, G. J. (2013). Temporal dynamics
447 in the free-living bacterial community composition in the coastal North Sea. *FEMS Microbiol. Ecol.*
448 83, 413–424. doi:10.1111/1574-6941.12003.

449 Spring, S., and Riedel, T. (2013). Mixotrophic growth of bacteriochlorophyll *a*-containing
450 members of the OM60/NOR5 clade of marine gammaproteobacteria is carbon-starvation
451 independent and correlates with the type of carbon source and oxygen availability. *BMC Microbiol.*
452 13, 117. doi:10.1186/1471-2180-13-117.

453 Šilović, T., Balagué, V., Orlić, S., and Pedrós-Alió, C. (2012). Picoplankton seasonal variation
454 and community structure in the northeast Adriatic coastal zone. *FEMS Microbiol. Ecol.* 82,
455 678–691. doi:10.1111/j.1574-6941.2012.01438.x.

456 Teeling, H., Fuchs, B. M., Becher, D., Klockow, C., Gardebrecht, A., Bennke, C. M., et
457 al. (2012). Substrate-controlled succession of marine bacterioplankton populations induced by a
458 phytoplankton bloom. *Science* 336, 608–611. doi:10.1126/science.1218344.

459 Teeling, H., Fuchs, B. M., Bennke, C. M., Krüger, K., Chafee, M., Kappelmann, L., et al.
460 (2016). Recurring patterns in bacterioplankton dynamics during coastal spring algae blooms. *eLife*
461 5, e11888. doi:10.7554/eLife.11888.

462 Tinta, T., Vojvoda, J., Mozetič, P., Talaber, I., Vodopivec, M., Malfatti, F., et al. (2015).
463 Bacterial community shift is induced by dynamic environmental parameters in a changing coastal
464 ecosystem (northern Adriatic, northeastern Mediterranean Sea) – a 2-year time-series study. *Environ.*
465 *Microbiol.* 17, 3581–3596. doi:10.1111/1462-2920.12519.

466 Vergin, K. L., Beszteri, B., Monier, A., Cameron Thrash, J., Temperton, B., Treusch, A. H., et al.
467 (2013). High-resolution SAR11 ecotype dynamics at the Bermuda Atlantic Time-series Study site
468 by phylogenetic placement of pyrosequences. *ISME J.* 7, 1322–1332. doi:10.1038/ismej.2013.32.

469 Ward, C. S., Yung, C.-M., Davis, K. M., Blinebry, S. K., Williams, T. C., Johnson, Z. I., et
470 al. (2017). Annual community patterns are driven by seasonal switching between closely related
471 marine bacteria. *ISME J.* 11, 1412–1422. doi:10.1038/ismej.2017.4.

472 Wickham, H. (2017). *tidyverse: Easily install and load the 'tidyverse'*.

- 473 Wickham, H., Averick, M., Bryan, J., Chang, W., McGowan, L. D., François, R., et al. (2019).
- 474 Welcome to the tidyverse. *J. Open Source Softw.* 4, 1686. doi:10.21105/joss.01686.
- 475 Wilke, C. O. (2019). *cowplot: Streamlined plot theme and plot annotations for 'ggplot2'*.
- 476 Xie, Y. (2014). “knitr: A comprehensive tool for reproducible research in R,” in *Implementing*
477 *Reproducible Computational Research*, eds. V. Stodden, F. Leisch, and R. D. Peng (New York:
478 Chapman and Hall/CRC), 3–32.
- 479 Xie, Y. (2015). *Dynamic Documents with R and knitr*. 2nd ed. Boca Raton, Florida: Chapman
480 and Hall/CRC.
- 481 Xie, Y. (2019a). *knitr: A general-purpose package for dynamic report generation in R*.
- 482 Xie, Y. (2019b). TinyTeX: A lightweight, cross-platform, and easy-to-maintain LaTeX
483 distribution based on TeX Live. *TUGboat* 40, 30–32.
- 484 Xie, Y. (2019c). *tinytex: Helper functions to install and maintain 'TeX Live', and compile*
485 *'LaTeX' documents*.
- 486 Xie, Y., Allaire, J. J., and Grolemund, G. (2018). *R Markdown: The Definitive Guide*. 1st ed.
487 Boca Raton, Florida: Chapman and Hall/CRC.
- 488 Yilmaz, P., Parfrey, L. W., Yarza, P., Gerken, J., Pruesse, E., Quast, C., et al. (2014). The
489 SILVA and "All-Species Living Tree Project (LTP)" taxonomic frameworks. *Nucleic Acids Res.* 42,
490 D643–D648. doi:10.1093/nar/gkt1209.
- 491 Zhu, H. (2019). *kableExtra: Construct complex table with 'kable' and pipe syntax*.

492 **Figure legends**

493 **Fig. 1.** (A) Principal Coordinates Analysis (PCoA) of Bray-Curtis distances based on OTU
494 abundances of bacterial and archaeal communities sampled in Saline and Funtana Bay. The
495 proportion of explained variation by each axis is shown on the corresponding axis in parentheses.
496 (B) Distance-Based Redundancy Analysis (db-RDA) of Bray-Curtis distances based on the same
497 community data sampled at the same locations and constrained by a set of environmental parameters
498 (T – temperature, S – salinity, PO_4^{3-} – orthophosphate, NH_4^+ – ammonium, NO_2^- – nitrite, NO_3^- –
499 nitrate, SiO_4^{4-} – orthosilicate, PM – particulate matter, Chl *a* – chlorophyll *a* and PA – prokaryotic
500 abundance). Scaling type 1 was selected for the biplot. The proportion of community data variation
501 explained by environmental variables (R_a^2) is stated on the biplot, while the proportion of community
502 data variation explained by each canonical axis is shown on the corresponding axis in parentheses.
503 Samples in both plots originating from the same station or same season are labeled in different
504 shape and color.

505 **Fig. 2.** Taxonomic classification and relative contribution of the most abundant ($\geq 1\%$) bacterial and
506 archaeal sequences in communities sampled in Saline and Funtana Bay. No Relative – sequences
507 without known relatives

508 **Fig. 3.** Taxonomic classification and relative contribution of the most abundant ($\geq 1\%$)
509 cyanobacterial sequences in communities sampled in Saline and Funtana Bay. The proportion
510 of cyanobacterial sequences in the total bacterial and archaeal community is given above the
511 corresponding bar.

512 **Fig. 4.** Taxonomic classification and relative contribution of the most abundant ($\geq 1\%$) sequences
513 within the *Bacteroidota* in communities sampled in Saline and Funtana Bay. The proportion of
514 sequences classified as *Bacteroidota* in the total bacterial and archaeal community is given above the
515 corresponding bar. NR – No Relative (sequences without known relatives within the corresponding
516 group)

517 **Fig. 5.** Taxonomic classification and relative contribution of the most abundant ($\geq 2\%$)
518 alphaproteobacterial sequences in communities sampled in Saline and Funtana Bay. The proportion
519 of alphaproteobacterial sequences in the total bacterial and archaeal community is given above the
520 corresponding bar. NR – No Relative (sequences without known relatives within the corresponding
521 group)

522 **Fig. 6.** Taxonomic classification and relative contribution of the most abundant ($\geq 1\%$)
523 gammaproteobacterial sequences in communities sampled in Saline and Funtana Bay. The
524 proportion of gammaproteobacterial sequences in the total bacterial and archaeal community is
525 given above the corresponding bar. NR – No Relative (sequences without known relatives within
526 the corresponding group)

527 **Figures**

27

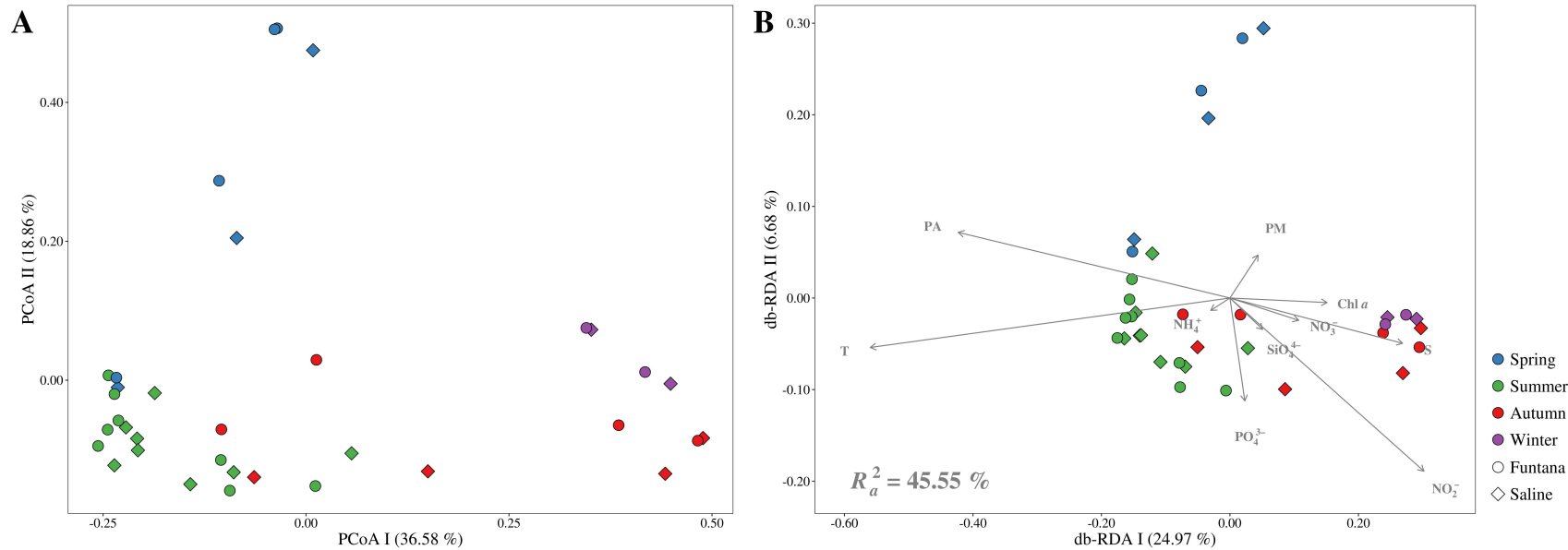


Fig. 1. (A) Principal Coordinates Analysis (PCoA) of Bray-Curtis distances based on OTU abundances of bacterial and archaeal communities sampled in Saline and Funtana Bay. The proportion of explained variation by each axis is shown on the corresponding axis in parentheses. (B) Distance-Based Redundancy Analysis (db-RDA) of Bray-Curtis distances based on the same community data sampled at the same locations and constrained by a set of environmental parameters (T – temperature, S – salinity, PO_4^{3-} – orthophosphate, NH_4^+ – ammonium, NO_2^- – nitrite, NO_3^- – nitrate, SiO_4^{4-} – orthosilicate, PM – particulate matter, Chl *a* – chlorophyll *a* and PA – prokaryotic abundance). Scaling type 1 was selected for the biplot. The proportion of community data variation explained by environmental variables (R_a^2) is stated on the biplot, while the proportion of community data variation explained by each canonical axis is shown on the corresponding axis in parentheses. Samples in both plots originating from the same station or same season are labeled in different shape and color.

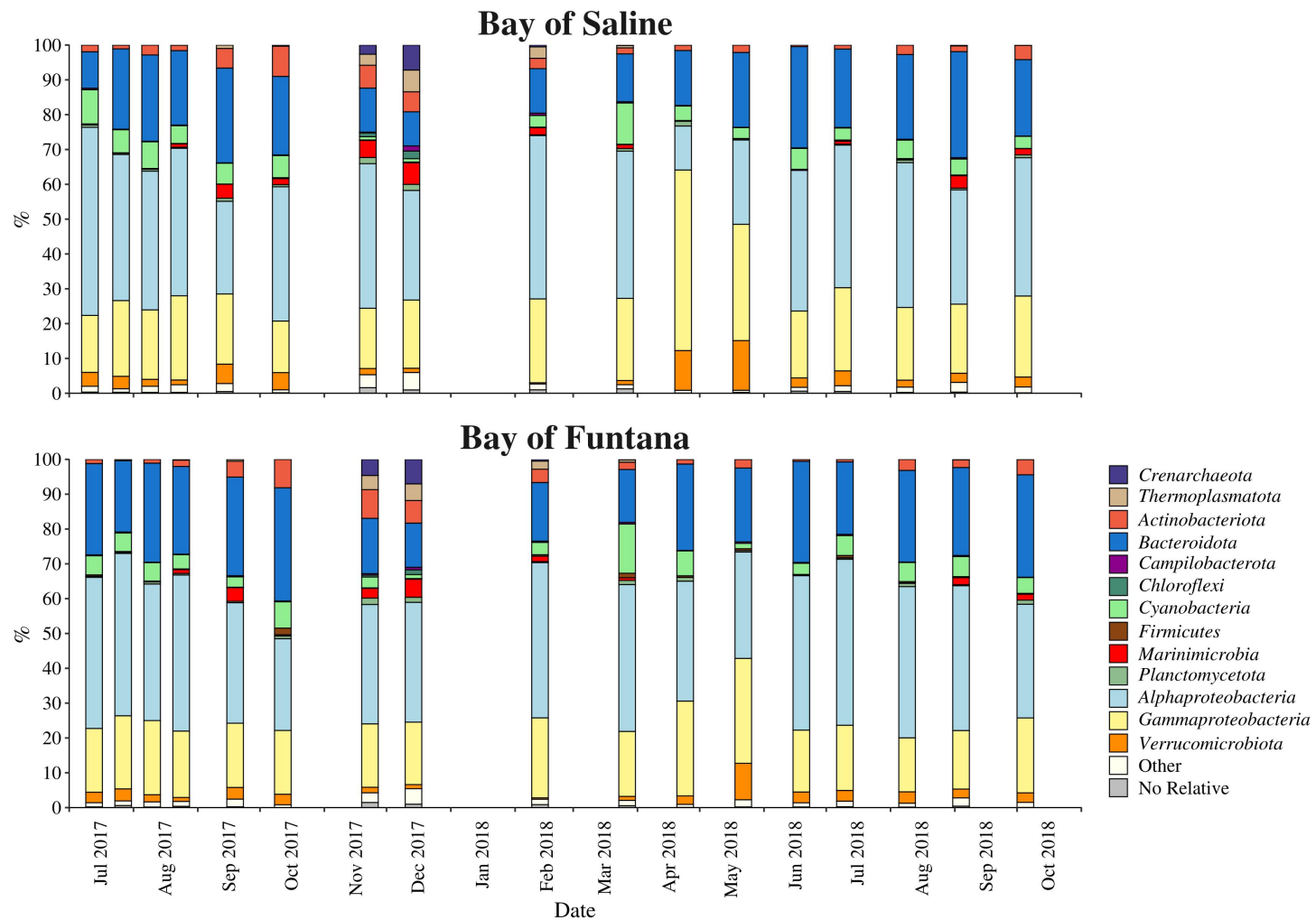


Fig. 2. Taxonomic classification and relative contribution of the most abundant ($\geq 1\%$) bacterial and archaeal sequences in communities sampled in Saline and Funtana Bay. No Relative – sequences without known relatives

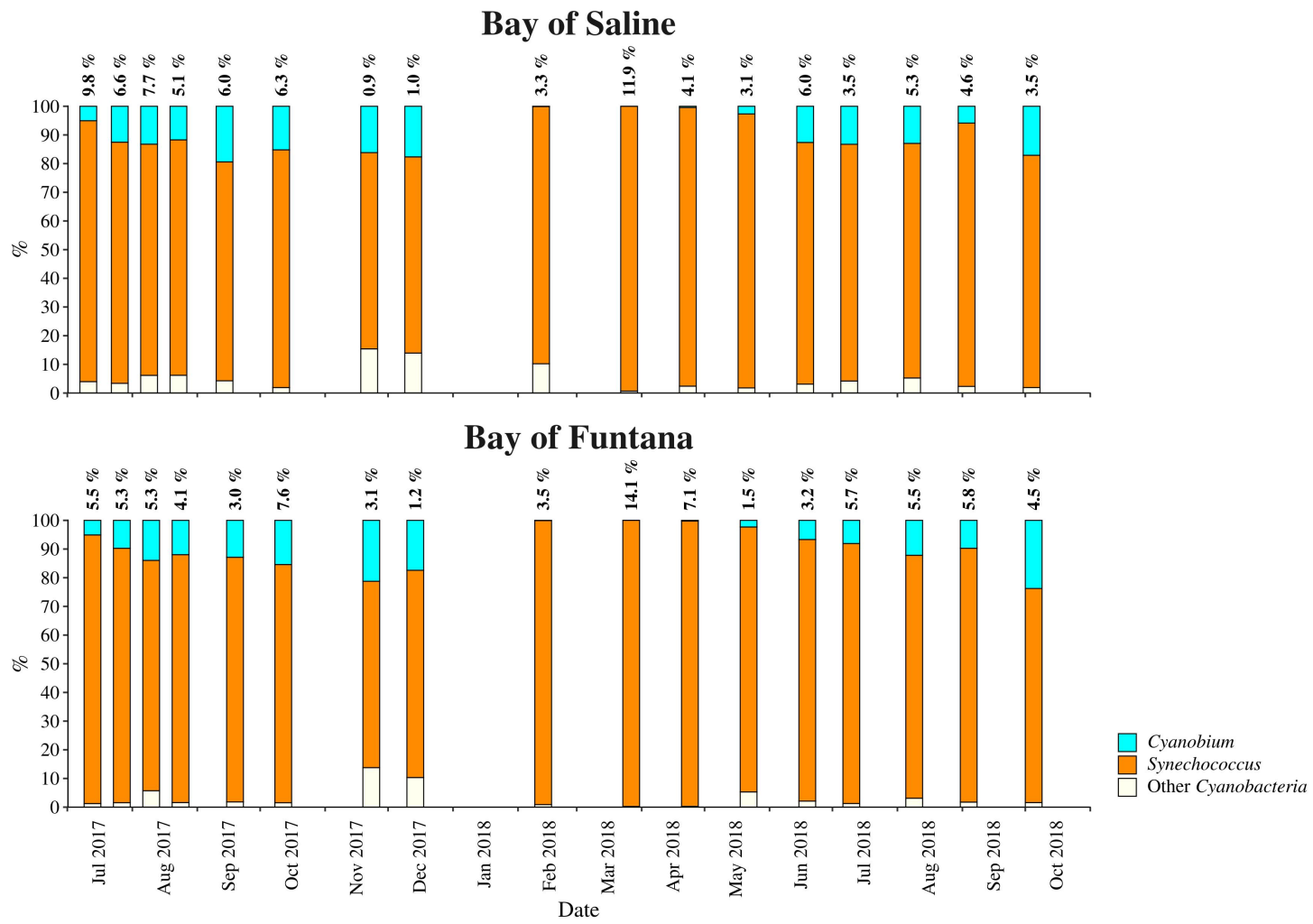


Fig. 3. Taxonomic classification and relative contribution of the most abundant ($\geq 1\%$) cyanobacterial sequences in communities sampled in Saline and Funtana Bay. The proportion of cyanobacterial sequences in the total bacterial and archaeal community is given above the corresponding bar.

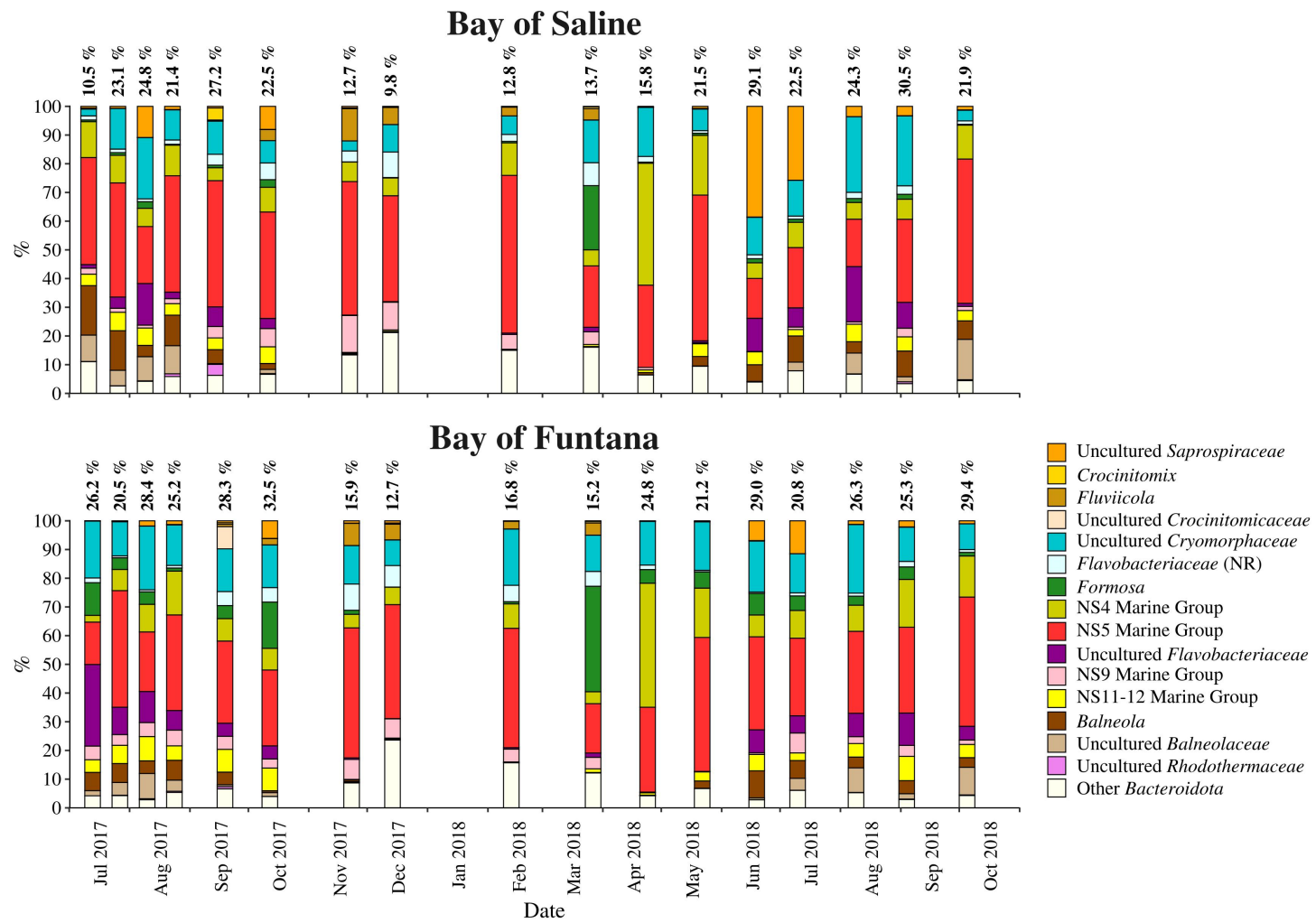


Fig. 4. Taxonomic classification and relative contribution of the most abundant ($\geq 1\%$) sequences within the *Bacteroidota* in communities sampled in Saline and Funtana Bay. The proportion of sequences classified as *Bacteroidota* in the total bacterial and archaeal community is given above the corresponding bar. NR – No Relative (sequences without known relatives within the corresponding group)

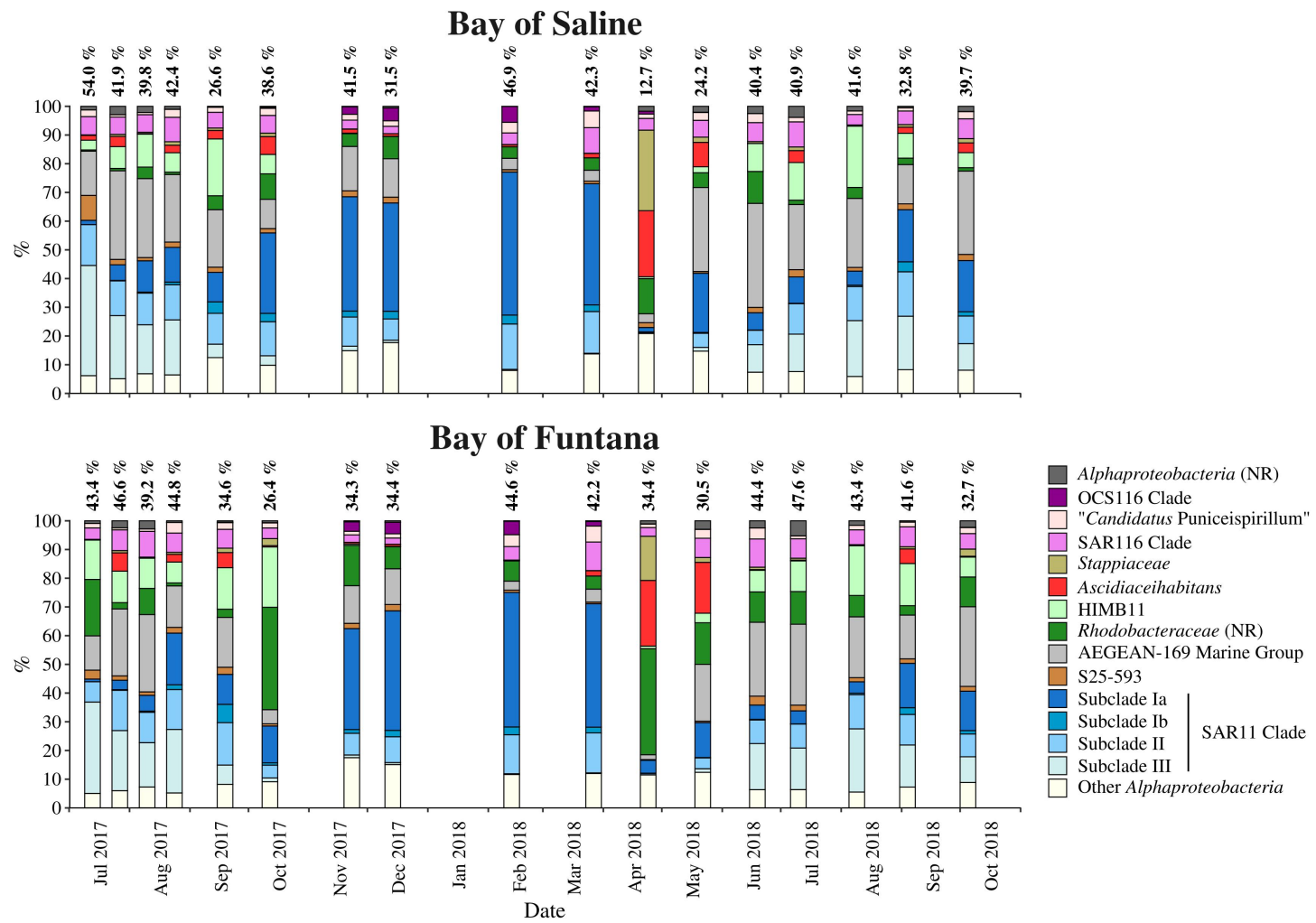


Fig. 5. Taxonomic classification and relative contribution of the most abundant ($\geq 2\%$) alphaproteobacterial sequences in communities sampled in Saline and Funtana Bay. The proportion of alphaproteobacterial sequences in the total bacterial and archaeal community is given above the corresponding bar. NR – No Relative (sequences without known relatives within the corresponding group)

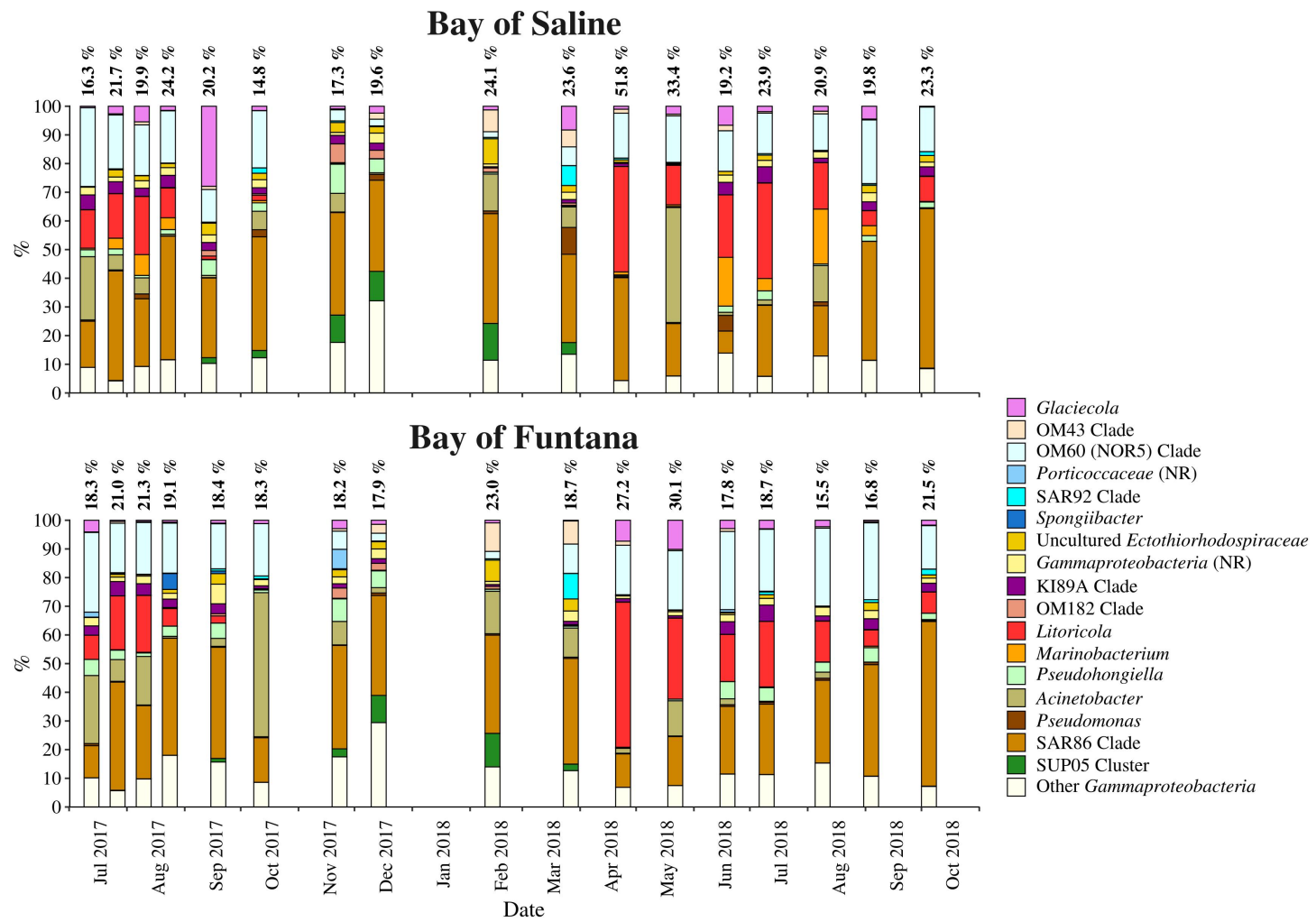


Fig. 6. Taxonomic classification and relative contribution of the most abundant ($\geq 1\%$) gammaproteobacterial sequences in communities sampled in Saline and Funtana Bay. The proportion of gammaproteobacterial sequences in the total bacterial and archaeal community is given above the corresponding bar. NR – No Relative (sequences without known relatives within the corresponding group)